On the Design of Irregular HetNets with Flow-Level Traffic Dynamics

Arman Shojaeifard*, Khairi Ashour Hamdi†, Emad Alsusa†, Daniel K. C. So†, Kai-Kit Wong*
*Department of Electronic and Electrical Engineering, University College London, London WC1E 7JE, United Kingdom
†School of Electrical and Electronic Engineering, University of Manchester, Manchester M13 9PL, United Kingdom
E-mail: {a.shojaeifard, kai-kit.wong}@ucl.ac.uk, {k.hamdi, e.alsusa, d.so}@manchester.ac.uk

***Abstract*—The application of stochastic geometry theory for the study of cellular networks has gained huge popularity recently. Most existing works however rely on unrealistic assumptions concerning the underlying user traffic model. This paper aims to make a step in this direction by devising a new model for the performance analysis and optimization of heterogeneous cellular networks (HetNets) with irregular BS deployment and flow-level traffic dynamics. We provide a unified methodology for the evaluation of the flow rate with closed-form expressions of the useful signal power and aggregate network interference over Nakagami-m fading channels. The problem of computing the optimal loading factors which result in the greatest sustainable traffic whilst the system remains stable is formulated and tackled.**

I. Introduction

Deterministic models, such as the hexagonal-grid and Wyner, have long served as de facto tools in the theoretical study of wireless communication networks. These abstraction topologies however cannot account for the inherently dense and irregular characteristics of emerging heterogeneous cellular networks (HetNets). To this end, tools from applied probability theory, in particular stochastic geometry and point processes, have recently been heavily utilized in the design and modeling of cellular systems.

Benign assumptions are however typically used for the sake of analytical tractability in the existing stochastic geometry-based models [1]. A major limitation is the notion that all base stations (BSs) are always-transmitting. In reality though, the activities of BSs depend on the load that the network is experiencing. Some papers, such as [2], have hence characterized the activities of BSs as a function of active user equipments (UEs) density (i.e., static traffic). This approach, whilst being an improvement over the fully-loaded system model, is nevertheless limited as in practical cases, UEs arrive randomly in time and space, initiate data communication flows, and leave the network once the job is completed [3].

The difficulty in adopting the impact of flow-level traffic dynamics arises from the interdependence between the transmitting sources density and the packet success probability [4]. This interaction has a paramount impact on traffic management issues, as shown in the context of distributed systems in [5], hexagonal-grid wireless networks in [6] and [7], and real-line cellular deployments in [8]. The study of flow-level traffic dynamics and related issues such as interference coordination and stability however remain largely unexplored for emerging HetNets with irregular BS deployment.

This paper makes a step in this direction by utilizing tools from stochastic geometry, queuing, and information theory to devise a framework for the study of generalized multi-tier cellular networks with elastic data traffic. Here, we consider a typical downlink wireless cell with a guard region surrounded by a dominant guard-edge interferer from each tier and an outer-bound Poisson field of heterogeneous interfering sources. The user arrivals in the system are modeled using an inhomogeneous Poisson point process (PPP). We present a moment-generating-function (MGF) methodology with closed-form expressions of the useful signal power and aggregate interference statistics over Nakagami-m fading channels for the evaluation of the flow rate. Finally, the traffic capacity defined as the maximum job densities for which the system remains unsaturated is derived and determined. The results reveal several useful design insights concerning traffic management issues in emerging HetNets.

Notation: $\mathbb{E}_{(.)}\{x\}$, $\mathscr{P}(x)$, $\mathcal{M}_x(.)$, and $\mathcal{P}_x(.)$ are the average value, probability, MGF, and probability density function (pdf) of x; $\Gamma(.)$ and $\Gamma(.,.)$ are the Gamma and incomplete Gamma functions; and ${}_2\tilde{F}_1(.,.;.;.)$ is the Regularized Gauss hypergeometric function, respectively.

II. System Model and Assumptions

We consider a hybrid HetNet topology, first proposed in [9] for the study of the interference statistics in cellular systems, where a typical circular-shaped downlink wireless cell is surrounded by an outer-bound heterogeneous interference field comprising of T-classes of BSs distributed via independent stationary PPPs $\Phi_t^{(b)}$ with spatial densities $\lambda_t^{(b)}$ and transmit powers p_t, where $t \in \mathcal{T} = \{1, 2, ..., T\}$. The serving BS of the reference cell under consideration is assumed to belong to the tier $h \in \mathcal{T}$ network with a probability [10]

$$\mathscr{P}_h = \frac{\lambda_h^{(b)}}{\sum_{t\in\mathcal{T}} \lambda_t^{(b)} \left(\frac{p_t}{p_h}\right)^{\frac{2}{\beta}}} \tag{1}$$

where β is used to denote the unbounded distance-dependent path-loss exponent. In order to capture the characteristics of a typical multiplicatively-weighted Voronoi cell, the radius of the reference cell is set to

$$r_{h,c} = \frac{1}{2\sqrt{\lambda_{h,\mathcal{T}}}} \tag{2}$$

where

$$\lambda_{h,\mathcal{T}} = \sum_{t\in\mathcal{T}} \left(1 + \left(\frac{p_t}{p_h}\right)^{\frac{1}{\beta}}\right)^2 \lambda_t^{(b)}. \quad (3)$$

A guard region for each tier-t network with the following radius is enforced from the cell boundary of the reference BS in order to guarantee that it provides the cell-edge users with the strongest received signal power:

$$r_{t,g} = \left(\frac{p_t}{p_h}\right)^{\frac{1}{\beta}} r_{h,c}. \quad (4)$$

The interference environment around the reference cell is assumed to further consist of one dominant source from each tier-t network uniformly-distributed at the respective tier-t guard region boundary [9].

To adopt the impact of flow-level traffic dynamics in the system, each BS is assumed to be represented by an independent M/G/1/PS queue: 'M' stands for Markovian-Poisson arrivals, 'G' denotes generally-distributed service times, '1' stands for single server, and 'PS' (processor sharing) corresponds to the equal allocation of capacity among users [3]. The number of active users arriving at location x is modeled by an inhomogeneous PPP of intensity $\lambda^{(u)}(x)\,\mathrm{d}x$ (flow/s). The serving tier-t BSs are required to transmit volumes of independent and identically-distributed (i.i.d.) data with mean $\frac{1}{\mu_t}$ (bits/flow) to their active users. The respective traffic demand in an area $\mathcal{A}_t$ in an arbitrary tier-t cell can be computed by $\rho_t = \frac{\overline{\lambda}_t^{(u)}}{\mu_t}$ (bits/s) where $\overline{\lambda}_t^{(u)} = \int_{\mathcal{A}_t} \frac{\lambda^{(u)}(x)}{\mathcal{A}_t}\,\mathrm{d}x$ (flow/s) is the respective average flow intensity in $\mathcal{A}_t$.

Let $Y_{h,0}$, $Y_{t,d}$, and $Y_{t,k}$ respectively denote the locations of the serving BS, the dominant tier-t interferer, and the k-th tier-t BS from the PPP-based interference field. Moreover, $r_{h,0}$, $r_{t,d}$, and $r_{t,k}$ are used to represent the distance from the serving BS, the dominant tier-t interferer, and the k-th tier-t BS from the PPP-based interference field to the reference user, respectively. Further, in the order given, $g_{Y_{h,0}}$, $g_{Y_{t,d}}$, and $g_{Y_{t,k}}$ correspond to the channel power gains at the receiver from the serving BS, the dominant tier-t interferer, and the k-th tier-t PPP-based source. Note that the notation $\psi_{Y_{t,i}}$ corresponds to a binary random variable depicting the activity of the tier-t BS located at $Y_{t,i}$. The probabilities of the interfering tier-t BS located at $Y_{t,i}$ being active and idle are denoted using $\rho_{Y_{t,i}} = \mathscr{P}\big(\psi_{Y_{t,i}} = 1\big)$ and $1 - \rho_{Y_{t,i}}$, respectively.

The corresponding signal-to-interference-plus-noise ratio (SINR) of the reference receiver at a distance $r_{h,0}$ from its serving tier-h BS in the reference cell under consideration can be written as [11]

$$\gamma_{h,0} = \frac{X_{h,0}}{I_{agg} + \eta} \quad (5)$$

where $X_{h,0}$, I_{agg}, and η respectively denote the received signal power, aggregate interference, and the variance of the additive white noise, respectively. The received signal power can be expressed as

$$X_{h,0} = p_h g_{Y_{h,0}} r_{h,0}^{-\beta} \quad (6)$$

The combined interference from the dominant interferers and the PPP-based heterogeneous interference field on the reference receiver can be formulated as

$$I_{agg} = \sum_{t\in\mathcal{T}} I_{t,d} + \sum_{t\in\mathcal{T}} \sum_{Y_k\in\Phi_t^{(b)}} I_{t,k}$$
$$= \sum_{t\in\mathcal{T}} p_t \psi_{Y_{t,d}} g_{Y_{t,d}} r_{t,d}^{-\beta} + \sum_{t\in\mathcal{T}} \sum_{Y_k\in\Phi_t^{(b)}} p_t \psi_{Y_{t,k}} g_{Y_{t,k}} r_{t,k}^{-\beta} \quad (7)$$

where $I_{t,d}$ and $I_{t,k}$ denote the interference from the dominant tier-t BS and the k-th tier-t PPP-based source, respectively.

III. Theoretical Analysis

Here, we present a unified MGF-based theoretical model for the performance analysis of an arbitrary downlink wireless cell in the traffic-aware HetNet paradigm.

The conditional flow rate of the reference receiver in b/s/Hz at a distance $r_{h,0}$ from its serving tier-h BS in the system under consideration can be expressed as follows [2]

$$\mathcal{C}_h(r_{h,0}, \rho_{Y_{t,d}}, \rho_{Y_{t,k}}) = \mathbb{E}\{\log_2(1+\gamma_{h,0})|r_{h,0}\} = \log_2(e)$$
$$\times \int_0^{+\infty} \big[\big(1 - \mathcal{M}_{X_{h,0}|r_{h,0}}(z)\big)\mathcal{M}_{I_{agg}|r_{h,0}}(z)\big] \frac{\exp(-z\eta)}{z}\,\mathrm{d}z \quad (8)$$

where $\mathcal{M}_{X_{h,0}|r_{h,0}}(z)$ and $\mathcal{M}_{I_{agg}|r_{h,0}}(z)$ are the MGFs of the useful signal and aggregate interference conditioned on the distance of reference UE-BS pair being $r_{h,0}$. We proceed by deriving expressions for the aforementioned metrics considering Gamma-distributed channel power gains with Nagakami-m fading parameter m_t for tier-t links.

Hence, the conditional MGF of the useful signal power can be written as

$$\mathcal{M}_{X_{h,0}|r_{h,0}}(z) = \exp\Big(-z p_h g_{Y_{h,0}} r_{h,0}^{-\beta}\Big) = \left(1 + \frac{z p_h}{m_h r_{h,0}^{\beta}}\right)^{-m_h}. \quad (9)$$

Furthermore, we can write the following for the conditional MGF of the aggregate interference on the reference receiver

$$\mathcal{M}_{I_{agg}|r_{h,0}}(z) = \prod_{t\in\mathcal{T}} \big(1 - \rho_{Y_{t,d}} + \rho_{Y_{t,d}} \mathcal{M}_{I_{t,d}|r_{h,0}}(z)\big)$$
$$\times \mathbb{E}\left\{ \prod_{Y_{t,k}\in\Phi_t^{(b)}} \big(1 - \rho_{Y_{t,k}} + \rho_{Y_{t,k}} \mathcal{M}_{I_{t,k}|r_{h,0}}(z)\big) \right\}$$
$$\overset{(a)}{=} \prod_{t\in\mathcal{T}} \Big(1 - \rho_t + \rho_t \mathbb{E}\Big\{\exp\Big(-z p_t g_{Y_{t,d}} r_{t,d}^{-\beta}\Big)\Big\}\Big)$$
$$\times \mathbb{E}\left\{ \prod_{Y_{t,k}\in\Phi_t^{(b)}} \Big(1 - \rho_t + \rho_t \mathbb{E}\Big\{\exp\Big(-z p_t g_{Y_{t,k}} r_{t,k}^{-\beta}\Big)\Big\}\Big) \right\} \quad (10)$$

where $\mathcal{M}_{I_{t,d}|r_{h,0}}(z)$ and $\mathcal{M}_{I_{t,k}|r_{h,0}}(z)$ are respectively the conditional statistics of interference from the dominant tier-t node and k-th tier-t PPP-based source and (a) follows from the assumption that all tier-t cells experience identical loads ρ_t.

Because of the asymmetric property of the distance to the closest tier-t interferer (given the corresponding distances to the closest and furtherest edges of the reference cell are respectively $r_{h,c}+r_{t,g}-r_{h,0}$ and $r_{h,c}+r_{t,g}+r_{h,0}$), we proceed by developing an upper-bound approximation of the interference from each tier-t network outside a ball of radius $r_{h,c}+r_{t,g}-r_{h,0}$ around the reference receiver.

Under this assumption, the conditional MGF of the dominant tier-t interferer over Nakagami-m fading channels can be expressed as in (11). Furthermore, the conditional statistics of the PPP-based interference from tier-t sources, $\mathcal{M}_{I_{t,\text{PPP}}|r_{h,0}}(z)$, over Nakagami-m fading channels can be derived as in (12) where (a) follows by considering the interference in a disk of radius ϱ around the victim receiver with the limit as $\varrho\to+\infty$; (b) is written conditioned on $\mathcal{N}_t$ being a Poisson random variable depicting the total number of PPP-based tier-t interfering sources where $Y_{t,a}$ and $g_{Y_{t,a}}$ respectively denote the location and channel from an arbitrary tier-t BS to the reference user; (c) is derived by utilizing the identity $\mathbb{E}_N\{x^N\}=\exp(-(1-x)\mathbb{E}_N\{N\})$ for a Poisson random variable N; (d) is written using the pdf of the distance of uniformly-distributed nodes in the disk of radius ϱ

$$\mathcal{P}_{r_{t,k}}(x)=\frac{2x}{\varrho^2-\left(r_{h,c}+r_{t,g}-r_{h,0}\right)^2},\quad r_{h,c}+r_{t,g}-r_{h,0}<x<\varrho; \tag{13}$$

(e) follows from taking the limit as $\varrho\to+\infty$; (f) is evaluated using integration by parts; finally, (g) is obtained by taking the average with respect to $g_{Y_{t,a}}$.

We now proceed with the analysis by utilizing the fact that the volume of data is proportional to the average of the reciprocal of the transmission rate

$$\frac{1}{\mu_h}=\mathbb{E}\Big\{\frac{1}{B\mathcal{C}_h(r_{h,0},\rho_t)}\Big\} \tag{14}$$

$$\mathcal{M}_{I_{t,d}|r_{h,0}}(z)=\mathbb{E}\Big\{\exp\Big(-zp_tg_{t,d}(r_{h,c}+r_{t,g}-r_{h,0})^{-\beta}\Big)\Big\}$$
$$=\frac{m_t^{m_t}}{\Gamma(m_t)}\int_0^{+\infty}g^{m_t-1}\exp\Big(-g\Big[zp_t(r_{h,c}+r_{t,g}-r_{h,0})^{-\beta}+m_t\Big]\Big)\,\mathrm{d}g=\left(\frac{m_t}{zp_t(r_{h,c}+r_{t,g}-r_{h,0})^{-\beta}+m_t}\right)^{m_t} \tag{11}$$

$$\mathcal{M}_{I_{t,\text{PPP}}|r_{h,0}}(z)\overset{(a)}{=}\lim_{\varrho\to+\infty}\mathbb{E}\left\{\prod_{Y_{t,k}\in\Phi_t^{(b)}}\Big(1-\rho_t+\rho_t\mathbb{E}\Big\{\exp\Big(-zp_tg_{Y_{t,k}}r_{t,k}^{-\beta}\Big)\Big\}\Big)\right\}$$
$$\overset{(b)}{=}\lim_{\varrho\to+\infty}\mathbb{E}_{\mathcal{N}_t}\left\{\Big(1-\rho_t+\rho_t\mathbb{E}_{r_{t,a},g_{Y_{t,a}}}\Big\{\exp\Big(-zp_tg_{Y_{t,a}}r_{t,a}^{-\beta}\Big)\Big\}\Big)^{\mathcal{N}_t}\right\}$$
$$\overset{(c)}{=}\lim_{\varrho\to+\infty}\exp\Big(-\pi\lambda_t^{(b)}\rho_t\Big(\varrho^2-\left(r_{h,c}+r_{t,g}-r_{h,0}\right)^2\Big)\Big(1-\mathbb{E}_{r_{t,a},g_{Y_{t,a}}}\Big\{\exp\Big(-zp_tg_{Y_{t,a}}r_{t,a}^{-\beta}\Big)\Big\}\Big)\Big)$$
$$\overset{(d)}{=}\lim_{\varrho\to+\infty}\exp\left(-\pi\lambda_t^{(b)}\rho_t\Big(\varrho^2-\left(r_{h,c}+r_{t,g}-r_{h,0}\right)^2\Big)\mathbb{E}_{g_{Y_{t,a}}}\left\{\int_{r_{h,c}+r_{t,g}-r_{h,0}}^{\varrho}\frac{2x\big[1-\exp\big(-zp_tg_{Y_{t,a}}x^{-\beta}\big)\big]}{\varrho^2-\left(r_{h,c}+r_{t,g}-r_{h,0}\right)^2}\,\mathrm{d}x\right\}\right)$$
$$\overset{(e)}{=}\exp\left(-\pi\lambda_t^{(b)}\rho_t\mathbb{E}_{g_{Y_{t,a}}}\left\{\int_{r_{h,c}+r_{t,g}-r_{h,0}}^{+\infty}2x\big[1-\exp\big(-zp_tg_{Y_{t,a}}x^{-\beta}\big)\big]\,\mathrm{d}x\right\}\right)$$
$$\overset{(f)}{=}\exp\Big(-\pi\lambda_t^{(b)}\rho_t\mathbb{E}_{g_{Y_{t,a}}}\Big\{\Big[\Gamma\Big(1-\tfrac{2}{\beta}\Big)-\Gamma\Big(1-\tfrac{2}{\beta},zp_tg_{Y_{t,a}}(r_{h,c}+r_{t,g}-r_{h,0})^{-\beta}\Big)\Big]\left(zp_tg_{Y_{t,a}}\right)^{\frac{2}{\beta}}$$
$$+\left(r_{h,c}+r_{t,g}-r_{h,0}\right)^2\Big(\exp\Big(-zp_tg_{Y_{t,a}}(r_{h,c}+r_{t,g}-r_{h,0})^{-\beta}\Big)-1\Big)\Big\}\Big)$$
$$\overset{(g)}{=}\exp\Bigg(-\pi\lambda_t^{(b)}\rho_t\Bigg[\left(r_{h,c}+r_{t,g}-r_{h,0}\right)^2\Bigg(\left(\frac{m_t}{zp_t(r_{h,c}+r_{t,g}-r_{h,0})^{-\beta}+m_t}\right)^{m_t}-1\Bigg)$$
$$+\Gamma\Big(m_t+\frac{2}{\beta}\Big)\Bigg(\frac{\Gamma\Big(1-\frac{2}{\beta}\Big)}{\Gamma(m_t)}\Big(\frac{zp_t}{m_t}\Big)^{\frac{2}{\beta}}-m_t\Bigg(\frac{m}{zp_t(r_{h,c}+r_{t,g}-r_{h,0})^{-\frac{2}{m_t}-\beta}}\Bigg)^{m_t}$$
$$\times{}_2\tilde{F}_1\Big(m_t+1,m_t+\frac{2}{\beta};m_t+\frac{2}{\beta}+1;-\frac{m_t}{zp_t(r_{h,c}+r_{t,g}-r_{h,0})^{-\beta}}\Big)\Bigg)\Bigg]\Bigg). \tag{12}$$

where B is the effective allocated bandwidth. Note that the pdf of the transmitter-receiver distance in the reference tier-h cell is given by

$$\mathcal{P}_{r_{h,0}}(x) = \frac{2x}{r_{h,c}^2},\ 0 < x < r_{h,c}. \tag{15}$$

Hence, the following non-linear expression of the traffic load experienced by an arbitrary tier-h cell can be formulated

$$\rho_h = \frac{\overline{\lambda}_h^{(u)}}{\pi r_{h,c}^2} \int_0^{r_{h,c}} \frac{2\pi x}{B\mathcal{C}_h(x,\rho_t)}\,\mathrm{d}x. \tag{16}$$

The normalized flow rate (in an arbitrary tier-h cell) for a given load ρ_h can therefore be written as

$$\tilde{\lambda}_h^{(u)} = \rho_h B r_{h,c}^2 \left(\int_0^{r_{h,c}} \frac{2x}{\mathcal{C}_h(x,\rho_t)}\,\mathrm{d}x \right)^{-1}. \tag{17}$$

On the other hand, it is well known from queuing theory that the probability of a stable tier-t BS (i.e., queue) transmitting must satisfy $0 < \rho_t < 1$ (finite stationary user distribution). The traffic capacity, defined as the maximum job densities for which the cells of different tiers remain unsaturated, can thus be formulated as

$$\tilde{\lambda}_{\text{opt}}^{(u)} = \sum_{h\in\mathcal{T}} \mathscr{P}_h \max_{0<\rho_h^*<1} \left[\frac{\rho_h^* r_{h,c}^2}{\int_0^{r_{h,c}} \frac{2x}{\mathcal{C}(x,\rho_t^*)}\,\mathrm{d}x} \right] \tag{18}$$

where ρ_t^* is used to denote the optimal loading factor for the tier-t cells. The above expression can be used to pinpoint the optimal load-balancing strategy for achieving the highest flow rate in the HetNet under consideration.

IV. Results and Discussions

Here, we consider a two-tier cellular network deployment comprising of large- and small-cells with state-of-the-art operational parameters (respectively denoted using subscripts l and s). Fig. 1 illustrates the corresponding HetNet flow rate, $\tilde{\lambda}^{(u)}$, for different probabilities of the high and low-power nodes being busy. In general, the total number of successfully transmitted packets per unit time and bandwidth in the reference cell first increases and then strictly decreases by increasing the small-cells loading factor. A similar trend can be observed for the impact of large-cells where the flow rate is a bell-shaped function in the high-power nodes transmission density. In the case of the fully-loaded large-cell-only system, however, increasing the small-cells loading factor continuously enhances the overall HetNet performance; the rate of improvement however drops as ρ_s moves away from zero. Under the particular set of system parameters considered here, the highest performance is achieved through a combination of large- and small-cells with relatively low and high loading factors, respectively. For example, from Fig. 1, the HetNet with $\rho_l = 0.25$ and $\rho_s = 0.6$ respectively achieves 22.56%, 32.72%, and 102.38% higher performance over the fully-loaded HetNet ($\rho_l = 1$ and $\rho_s = 1$), small-cell-only ($\rho_l = 0$ and $\rho_s = 1$), and large-cell-only ($\rho_l = 1$ and $\rho_s = 0$) counterparts. This trend highlights the promising potential of HetNets with small-cell solution over conventional single-tier deployments towards meeting the increasingly high system throughput requirements. It is important to note that, overall, the results produced by our proposed model provide a near-exact fit to those from the Monte-Carlo simulations whilst requiring significantly less resources for computation.

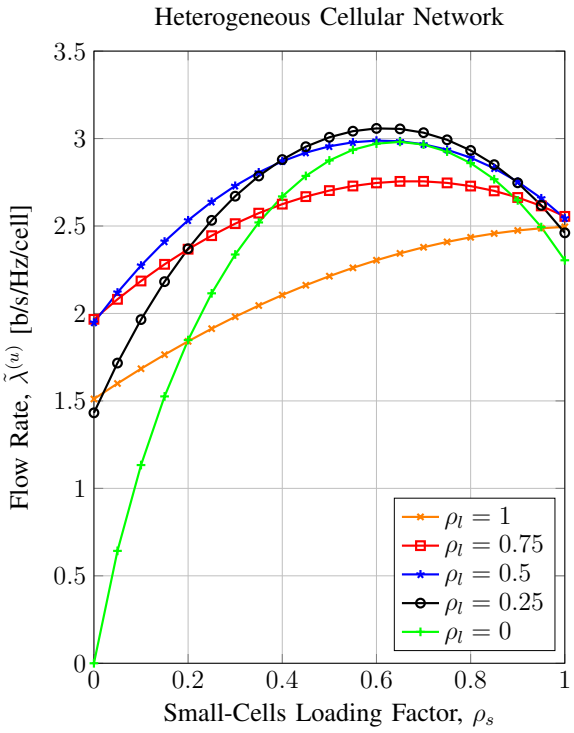

Fig. 1: System parameters are: $p_l = 20$ W, $p_s = 0.1$ W, $m_l = 1$, $m_s = 2$, $\lambda_l^{(b)} = 0.5$ BSs/km^2, $\lambda_s^{(b)} = 2$ BSs/km^2, $\beta = 6$, $\frac{1}{\eta} = 20$ dB. Theoretical and simulation results are respectively depicted by solid lines and markers.

Next, we turn our attention to the problem of pinpointing the optimal loading factors required for achieving the traffic capacity in the HetNet under consideration. In order to tackle the non-linear constrained multidimensional optimization problem, we employ the heuristic downhill simplex method [12] with penalty function which is typically solvable in exponential time [13]. The traffic capacity and the corresponding optimal loading factors in the two-tier system considered are captured for a wide range of noise values in Fig. 2. It can be observed that in noise-limited scenarios, the traffic capacity is achieved by setting the queue transmission probabilities of the large- and small-cells to one. As the noise variance relative to the transmit power is reduced, however, the optimal loading factors of the different tiers go down and the traffic capacity increases. Note that the rate of decrease is steeper for the high-power nodes, e.g., by increasing the noise inverse variance from -10 dB to 0 dB, ρ_l^* and ρ_s^* respectively decrease by 36.20% and 21.44%. In interference-limited scenarios, the traffic capacity along with the respective optimal loading factors of the different tiers reach a plateau. A similar trend can

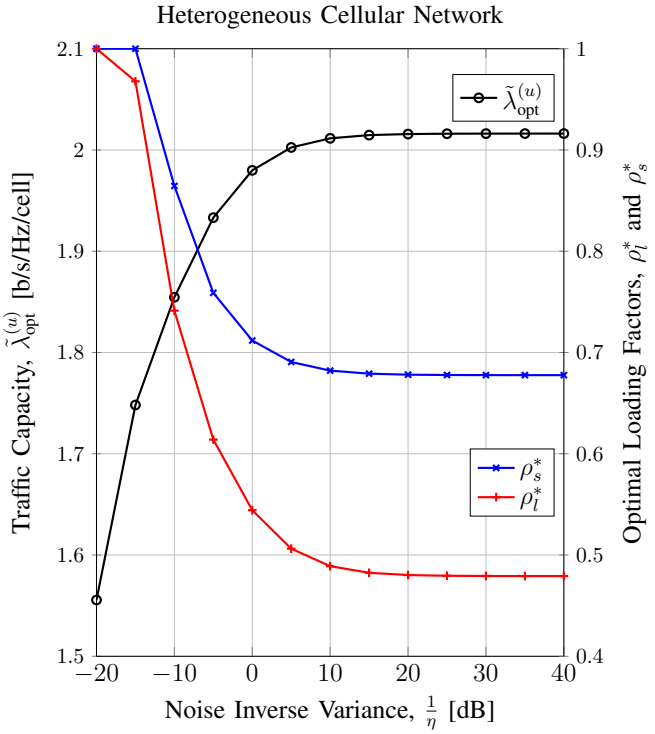

Fig. 2: System parameters are: $p_l = 20$ W, $p_s = 0.1$ W, $m_l = 1$, $m_s = 2$, $\lambda_l^{(b)} = 0.2$ BSs/km^2, $\lambda_s^{(b)} = 1$ BSs/km^2, $\beta = 4$. Theoretical and simulation results are respectively depicted by solid lines and markers.

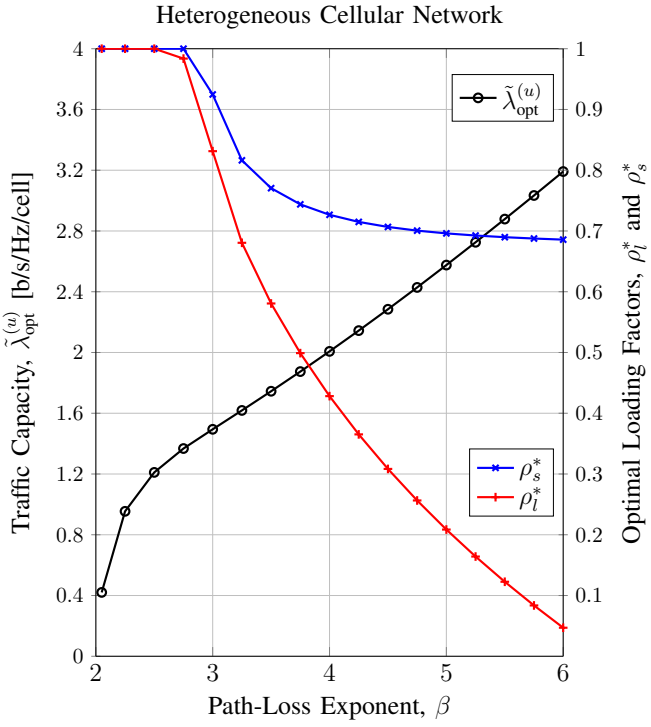

Fig. 3: System parameters are: $p_l = 20$ W, $p_s = 0.1$ W, $m_l = 1$, $m_s = 2$, $\lambda_l^{(b)} = 0.25$ BSs/km^2, $\lambda_s^{(b)} = 2.5$ BSs/km^2, $\frac{1}{\eta} = 0$ dB. Theoretical and simulation results are respectively depicted by solid lines and markers.

be observed for the HetNet performance under different path-loss exponents in Fig. 3. The traffic capacity, however, almost linearly improves in more favourable distance-dependent path-loss conditions. The optimal loading factors of the different tiers in turn continue to drop as β moves away from (near) two. The rate of decrease in the transmission density of high-power nodes is significantly higher over that of the small-cells, indicating the major benefit of the small-cell-solution in interference-limited cellular environments.

V. Conclusions

In this paper, we introduced a unified framework using tools from stochastic geometry and queuing theory for the performance analysis of HetNets with irregular BS deployment and flow-level traffic dynamics. A non-direct MGF-based approach for the calculation of the flow rate with closed-form expressions of the useful signal power and aggregate interference statistics over Nakagami-m fading channels was provided. The problem of finding the optimal loading factors for which the greatest sustainable elastic data traffic load is supported whilst satisfying the system stability condition was mathematically formulated and solved numerically. The results revealed several useful design insights concerning traffic management issues in emerging multi-tier cellular networks.

References

[1] J. Andrews, S. Singh, Q. Ye, X. Lin, and H. Dhillon, "An overview of load balancing in HetNets: old myths and open problems," *IEEE Trans. Wireless Commun.*, vol. 21, no. 2, pp. 18–25, Apr. 2014.

[2] A. Shojaeifard, K. Hamdi, E. Alsusa, D. So, and J. Tang, "A unified model for the design and analysis of spatially-correlated load-aware HetNets," *IEEE Trans. Commun.*, vol. 62, no. 11, pp. 1–16, Nov. 2014.

[3] R. Combes, Z. Altman, and E. Altman, "Interference coordination in wireless networks: A flow-level perspective," in *INFOCOM, 2013 Proceedings IEEE*, Apr. 2013, pp. 2841–2849.

[4] K. Stamatiou and M. Haenggi, "Random-access poisson networks: Stability and delay," *IEEE Commun. Lett*, vol. 14, no. 11, pp. 1035–1037, Nov. 2010.

[5] W. Luo and A. Ephremides, "Stability of N interacting queues in random-access systems," *IEEE Trans. Inform. Theory*, vol. 45, no. 5, pp. 1579–1587, Jul. 1999.

[6] M. Karray and M. Jovanovic, "A queueing theoretic approach to the dimensioning of wireless cellular networks serving variable-bit-rate calls," *IEEE Trans. Veh. Technol.*, vol. 62, no. 6, pp. 2713–2723, Jul. 2013.

[7] F. Baccelli, B. Blaszczyszyn, and M. K. Karray, "Blocking rates in large CDMA networks via a spatial Erlang formula," in *INFOCOM 2005. 24th Annual Joint Conference of the IEEE Computer and Communications Societies. Proceedings IEEE*, vol. 1, Mar. 2005, pp. 58–67 vol. 1.

[8] K. Stamatiou and M. Haenggi, "Traffic management in random cellular networks," in *Information Theory and Applications Workshop (ITA), 2014*, Feb. 2014, pp. 1–5.

[9] R. Heath and M. Kountouris, "Modeling heterogeneous network interference," in *Information Theory and Applications Workshop (ITA), 2012*, Feb. 2012, pp. 17–22.

[10] A. Shojaeifard, K. Hamdi, E. Alsusa, D. K. C. So, J. Tang, and K. K. Wong, "Design, modeling, and performance analysis of multi-antenna heterogeneous cellular networks," *IEEE Trans. Commun.*, accepted 2016.

[11] A. Shojaeifard, K. Hamdi, E. Alsusa, D. So, and J. Tang, "Exact SINR statistics in the presence of heterogeneous interferers," *IEEE Trans. Inform. Theory*, vol. 61, no. 12, pp. 6759–6773, Dec. 2015.

[12] J. A. Nelder and R. Mead, "A simplex method for function minimization," *Computer Journal*, vol. 7, pp. 308–313, 1965.

[13] S. Singer and S. Singer, "Efficient implementation of the Nelder-Mead search algorithm," *Applied Numerical Analysis and Computational Mathematics*, vol. 1, no. 2, pp. 524–534, 2004.